

Simulation of the A – X and B – X transition emission spectra of the InCl molecule in low pressure plasmas

S. Briefi^{a,b,*}, U. Fantz^{a,b}

^a*Lehrstuhl für Experimentelle Plasmaphysik, Universität Augsburg, Universitätsstr. 1, 86135 Augsburg, Germany*

^b*Max-Planck-Institut für Plasmaphysik, EURATOM Association, Boltzmannstr. 2, 85748 Garching, Germany*

Abstract

Low pressure plasmas containing indium halides as radiators are discussed for lighting applications as efficient alternative to mercury-containing fluorescent lamps. To gain insight in plasma parameters like the vibrational and rotational temperature of the molecule, the near UV emission spectra of the indium halides arising from the A $^3\Pi_{0+} \rightarrow X ^1\Sigma^+$ and the B $^3\Pi_1 \rightarrow X ^1\Sigma^+$ transitions are simulated. Such a simulation requires Franck-Condon factors and vibrationally resolved transition probabilities which are not available in the literature for InCl. Therefore, they have been calculated by solving the Schrödinger equation using the Born-Oppenheimer approximation. The values of the Franck-Condon factors and the transition probabilities are presented. For the A – X transition a good match of the simulated and measured spectra could be achieved but for the B – X transition neither the relative intensity nor the wavelength could be reproduced. This indicates that for the B state the values of the molecular constants, the potential curve and/or the electronic dipole transition moment of the B – X transition are inaccurate. Despite this mismatch the rotational and vibrational temperatures of the molecule can still be determined using the A – X transition.

Keywords: Indium chloride, Molecular emission, Franck-Condon factors, Transition probabilities

1. Introduction

The utilization of indium halides as radiator in low pressure discharges is discussed as efficient alternative to common fluorescent lamps which contain hazardous mercury [1]. The desired emission is located in the near UV spectral range between 300 and 400 nm which allows for a small Stokes shift (the energy lost in the conversion process of UV into visible light by means of a phosphor).

*Corresponding author

Email address: stefan.briefi@physik.uni-augsburg.de (S. Briefi)

The emission arises from both the $A \ ^3\Pi_{0+} \rightarrow X \ ^1\Sigma^+$ and the $B \ ^3\Pi_1 \rightarrow X \ ^1\Sigma^+$ transition (an exemplary emission spectrum of InCl is shown in figure 1). Investigations of InBr, InCl and InI already proved the high efficiency of such a kind of discharge lamp [2]. However, in order to maximize the near UV radiation systematically, the population mechanisms of the molecular states involved in the desired transitions have to be investigated. This can be achieved by simulating the relative emission spectra and fitting it to the measured spectrum [3]. Such a simulation calculates the vibrational and rotational population based on molecular constants, Franck-Condon factors and vibrationally resolved transition probabilities. For InBr such a simulation has already been realized successfully [4].

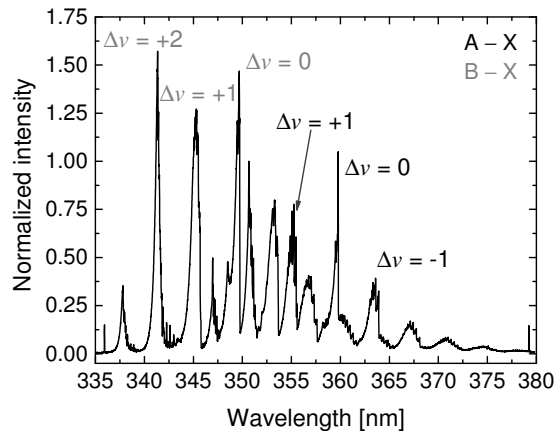


Figure 1: Exemplary near UV emission spectrum of InCl arising from the $A - X$ and the $B - X$ transition. Some exemplary sequences $\Delta v = v' - v''$ of the electronic transitions are labelled.

In this paper the simulation of the emission spectrum is carried out for the InCl molecule. In general it is based on the same computing method as for InBr, but the molecule-specific parameters such as molecular constants, Franck-Condon factors and transition probabilities are substituted. For InCl neither Franck-Condon factors nor vibrationally resolved transition probabilities can be found in the literature. Therefore this data was calculated from potential curves and electronic dipole transition moments using the program TraDiMo [5]. The input parameters and the results of this calculation are described in section 2. The comparison of simulated and measured spectra is carried out in section 3.

2. Simulation of the emission spectrum

Only a brief description of the calculation method is given here, the reader is referred to [4] for a more detailed explanation. The simulation of the InCl emission is based on the calculation of the vibrational and rotational populations

of the electronic ground state X and the first two excited electronic states A and B assuming Boltzmann distributions with the vibrational temperature T_{Vib} and the rotational temperature T_{Rot} . The assumption of such a distribution is reasonable as the energy difference of the single vibrational and rotational states ($\Delta E_{Vib} \approx 0.03$ eV, $\Delta E_{Rot} \approx 3 \times 10^{-5}$ eV) is low compared to the gas temperature (typically above 800 K) or the electron temperature (typically just below 1 eV). The first 25 vibrational states and the first 300 rotational states of each electronic state are included in the calculations as this proved to be necessary to achieve a good match between simulation and measurement for the InBr molecule [4].

The vibrational population is calculated in the electronic ground state and transferred to the A or B state by applying Franck-Condon factors. This corresponds to a population of the excited states by electron impact excitation out of the ground state. As the redistribution of the rotational population in the excited electronic state via collisions with the background gas happens on a much shorter time scale than the radiative decay [6], the rotational population can be calculated directly in the excited electronic states. The relative intensity of the emission is then derived from the calculated population in the excited rovibronic state, the vibrationally resolved transition probabilities, the Hönl-London factors and constants of the particular transition such as statistical weights and the frequency of the emission line. For each emission line a Gaussian line profile having the full width at half maximum of the apparatus profile is calculated and folded with the relative intensity of the line. By adding up all emission lines from both the A – X and the B – X transition, the simulated spectrum is obtained.

As mentioned above, the simulation requires molecular constants, Franck-Condon factors and vibrationally resolved transition probabilities as input parameters. As these parameters are isotope-specific, the isotopes of InCl having a relevant natural abundance must be considered in the simulation. The two isotopes $^{115}\text{In}^{35}\text{Cl}$ and $^{115}\text{In}^{37}\text{Cl}$ (natural abundance 72.51% and 23.20% resp.) are taken into account whereas the isotopes $^{113}\text{In}^{35}\text{Cl}$ and $^{113}\text{In}^{37}\text{Cl}$ (3.25% and 1.04% resp.) are neglected due to their low abundance.

The molecular constants of InCl are taken from [7] which is a recent review of the spectroscopic constants of the diatomic indium halide molecules. However, Franck-Condon factors (FCF) and vibrationally resolved transition probabilities $A_{ik}^{v'v''}$ (i denotes the upper electronic state, v' the upper vibrational state, k and v'' the corresponding lower states) are not available in the literature for InCl. Therefore they have been calculated using the program TraDiMo which derives the eigenvalues and vibrational wave functions via numerically solving the Schrödinger equation (for a detailed description of the program see [5]). The calculations require Born-Oppenheimer potential curves, electronic dipole transition moments and the reduced mass of the molecule as input parameters. The overlap integral of two vibrational wave functions in different electronic states yields the FCF whereas the $A_{ik}^{v'v''}$ are calculated from the overlap of the vibrational wave functions with the electronic dipole transition moments.

Four different sets of potential curves for the relevant states of InCl are avail-

able: RKR potential curves [7], potential curves from two different quantum mechanical calculations [8, 9] and those obtained by a pseudopotential approximation [10]. As the data for RKR potential curves are only available up to a vibrational quantum number of 16 they are fitted using Morse potential curves which can be derived using molecular constants taken from [7]. The electronic dipole transition moments are given by [8] or by [11]. TraDiMo calculations were carried out with each possible set of potential curves and dipole transition moments for both relevant isotopes of InCl.

As the different potential curves and dipole transition moments deviate from each other, the obtained sets of FCF and $A_{ik}^{v'v''}$ and therefore also the simulated spectra show deviations. Simulations were carried out with all sets of obtained FCF and $A_{ik}^{v'v''}$ and compared to measured emission spectra. For the A – X transition a satisfying agreement of simulated and measured spectra could only be achieved with the data derived using the Morse potential curves and the electronic dipole transition moments of [11]. For the B – X transition the relative intensity and the wavelengths of the emission lines could not be reproduced properly with any parameter set. The smallest deviation between simulation and measurement was achieved by using the FCF and $A_{ik}^{v'v''}$ obtained from the Morse potential curves and the electronic dipole transition moments of [11]. An exemplary comparison of simulation and measurement demonstrating the deviations is shown in section 3. Possible reasons of the mismatch of the B – X transition are also discussed in this section.

As the calculation of Morse potential curves is based on molecular constants slightly different curves are obtained for each isotope which also lead to slightly different values of the determined FCF and $A_{ik}^{v'v''}$. Similar to the InBr simulation [4], TraDiMo calculations have been carried out on the one hand considering the mass of both relevant InCl isotopes and on the other hand with the averaged mass. The simulation results obtained by considering the isotopic composition for the Franck-Condon factors and the transition probabilities and by using the data obtained at the averaged mass only differs in the range of a few per cent. Therefore the FCF and $A_{ik}^{v'v''}$ obtained with the averaged mass are used in the simulation for simplicity (the corresponding Morse potential curves are shown in figure 2). The values are given in tables A.1 to A.8 in the Appendix. Considering the uncertainty of the obtained absolute values (a detailed discussion can be found in [4]), Franck-Condon factors that are smaller than 1×10^{-5} and transition probabilities smaller than 1 s^{-1} have been replaced by zero.

3. Comparison of simulated and measured spectra

Figure 3 shows a sketch of the experimental setup used for the measurements of the emission spectra. Discharges are generated in sealed cylindrical vessels (diameter 2.5 cm, length 18 cm) via inductive RF coupling at a frequency of 13.56 MHz and a power of 100 W. The vessels are filled with argon at a pressure of one mbar and a few mg of InCl salt. As the vapour pressure of InCl is very low at ambient temperature, the discharge vessel is placed in a heat container made out of aerated autoclaved concrete and heated up to several hundred

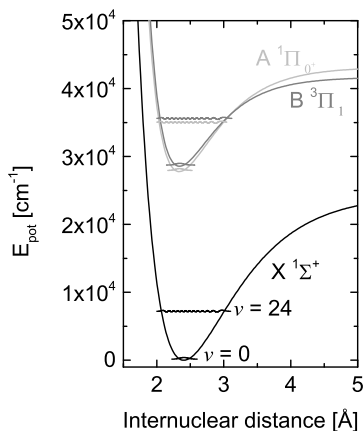


Figure 2: Morse potential curves of the X, A and B states utilized for the calculation of the FCF and $A_{ik}^{v'v''}$. The vibrational wavefunctions of the states with $v = 0$ and $v = 24$ calculated with the program TraDiMo are also shown.

degrees with hot air. In order to control the evaporated amount of the indium halide, a setup has been realized where the cold spot location is well-defined and the cold spot temperature (which determines the indium halide density in gas phase) is adjustable. For details on the setup and its performance see [12]. The optical emission spectroscopy measurements are performed at an axial (radial centred) line-of-sight (LOS) utilizing a wavelength and intensity calibrated high resolution spectrometer equipped with a CCD detector (focal length 750 mm, grating 1800 lines/mm). The full width at half maximum of the apparatus profile is 25 pm at 370 nm. Such a high spectral resolution is necessary in order to allow for a determination of the vibrational and the rotational temperature with high accuracy [4]. However, it should be noted that the single emission lines always overlap as the line width determined by natural, pressure and Doppler broadening is larger than the wavelength separation of the individual lines. Therefore, the high resolution is required to resolve the detailed structure of the whole band and not to resolve the single rotational branches.

Figure 4 shows an exemplary emission spectrum obtained from an InCl containing argon discharge at a cold spot temperature of 221 °C together with a simulation. The spectra are normalized to the maximum intensity of the $\Delta v = v' - v'' = +2$ sequence of the A – X transition. It can be seen that the A – X transition (which is primarily located above 350 nm) is reproduced quite well whereas neither the wavelength nor the relative intensity of the B – X transition (mainly located below 350 nm) matches the measurement. Looking at the spectra in more detail the mismatch of the $\Delta v = +3, +2$ and $+1$ sequences of the B – X transition is obvious (figure 5 a)) whereas even the details of the $\Delta v = +1$ sequence of the A – X transition are reproduced very well (see figure

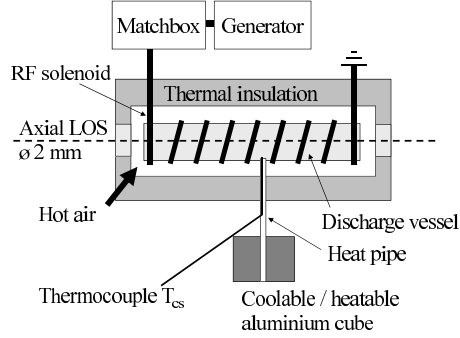


Figure 3: Sketch of the experimental setup.

5 b)).

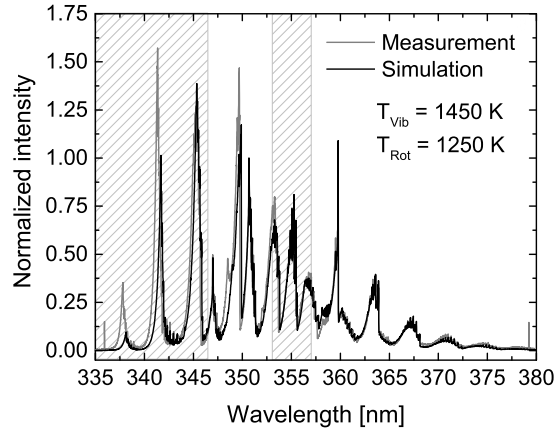


Figure 4: Measurement and simulation of an exemplary InCl emission spectrum. The parameters of the simulation are: $T_{Vib} = 1450 \pm 50$ K, $T_{Rot} = 1250 \pm 50$ K (determined from the A – X transition). The two highlighted parts of the spectrum are shown in figure 5 in more detail.

In figure 6 the simulated $\Delta v = +1$ sequence of the A – X transition is shown for a variation of the vibrational and of the rotational temperature. It can be seen that the vibrational temperature primarily determines the relative intensity of the whole sequence whereas the rotational temperature mainly influences the relative intensity in the left edge of the sequence. Due to the good reproduction of the measurement by the simulation concerning the A – X transition and especially the $\Delta v = +1$ sequence, the vibrational and rotational temperatures can be determined with high accuracy. The error can be estimated to be $\Delta T_{Vib} = \Delta T_{Rot} = \pm 50$ K.

In order to discuss possible reasons for the deviation of the wavelength posi-

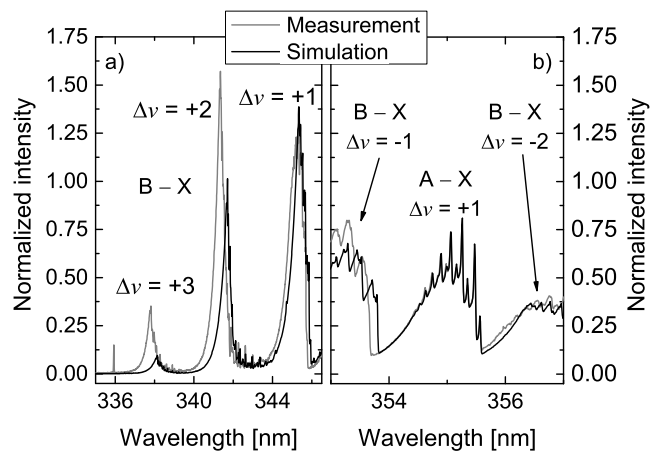


Figure 5: Details of the same spectrum as shown in figure 4. It can be seen that the simulation reproduces even the details of the A - X transition very well in contrast to the B - X transition.

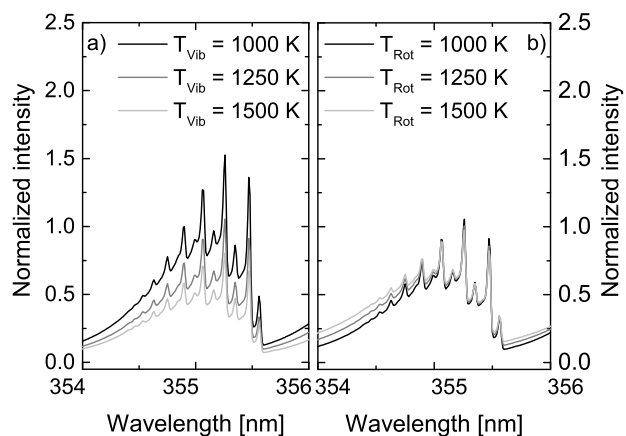


Figure 6: Simulation of the $\Delta v = +1$ sequence of the A - X transition with different values of T_{Vib} at a fixed rotational temperature of 1000 K (left part) and with different values of T_{Rot} at a fixed vibrational temperature of 1000 K (right part).

tion and of the relative intensity of the B – X transition, the input parameters of the simulation which influence these quantities have to be considered. The wavelength of the particular emission lines is calculated using only molecular constants of the involved electronic states. Therefore, the mismatch between simulation and measurement regarding the wavelength position can be assigned to be caused by the molecular constants. As the wavelength position of the A – X transition is reproduced well, it can be assumed that the molecular constants of the X state are correct and the deviation has to be caused by inaccurate molecular constants of the B state. The mismatch of the relative intensity of the simulated emission can be caused on the one hand by inaccurate potential curves and on the other hand by an inaccurate electronic dipole transition moment for the B – X transition. Again, as the A – X transition is reproduced well, the assumption can be made that the potential curve of the X state is accurate. This narrows the possible causes for the deviation down to inaccuracies of the potential curve of the B state or of the electronic dipole transition moment of the B – X transition.

4. Conclusion

Indium halides are discussed for lighting purposes as efficient alternative to hazardous mercury containing fluorescent lamps. To optimize the efficiency, insight in the molecular population processes is highly desirable. In order to achieve this goal a simulation of the relative intensity of the emission spectrum can be carried out. This simulation requires Franck-Condon factors and vibrationally resolved transition probabilities which were not available in the literature for InCl. Therefore this data has been calculated using the program TraDiMo and different sets of potential curves and electronic dipole transition moments as input parameters. The best match between measured spectra and simulated ones has been achieved for the data derived from Morse potential curves and electronic dipole transition moments taken from [11]. Using this input data which is presented in the tables in the appendix, the simulation can be fitted to the measurement for the A – X transition very well (especially to the $\Delta v = +1$ sequence) whereas the B – X transition shows deviations concerning the wavelength position and the relative intensity.

In summary, it has been demonstrated that the adjustment of the simulation to the measured InCl emission spectrum is suitable for determining the vibrational and rotational temperature of the InCl molecule if the A – X transition is considered.

References

- [1] Kitsinelis S, Zissis G, Fokitis E. A strategy towards the next generation of low pressure discharge lamps: lighting after mercury. *Journal of Physics D Applied Physics* 2009;42(4):045209 (pages 8).

- [2] Hayashi D, Hilbig R, Körber A, Schwan S, Scholl R, Boerger M, et al. Low-pressure indium-halide discharges for fluorescent illumination applications. *Applied Physics Letters* 2010;96(6):061503 (pages 2).
- [3] Fantz U. Basics of plasma spectroscopy. *Plasma Sources Science and Technology* 2006;15(4):S137–47.
- [4] Briefi S, Fantz U. Simulation of the A – X and B – X transition emission spectra of the InBr molecule for diagnostics in low-pressure plasmas. *Journal of Physics D: Applied Physics* 2011;44(15):155202 (pages 3).
- [5] Fantz U, Wunderlich D. Franck Condon factors, transition probabilities, and radiative lifetimes for hydrogen molecules and their isotopomers. *Atomic Data and Nuclear Data Tables* 2006;92:853–973.
- [6] Mulders HCJ. Spectroscopic Investigation of Indium Bromide for Lighting Purposes; 2010. PhD thesis, Eindhoven University of Technology.
- [7] Mishra SK, Yadav RKS, Singh VB, Rai SB. Spectroscopic Studies of Diatomic Indium Halides. *Journal of Physical and Chemical Reference Data* 2004;33:453–70.
- [8] Banerjee A, Das KK. Low-lying electronic states and spectroscopic properties of InCl and InCl⁺. *Journal of Molecular Structure: THEOCHEM* 2008;851:134–46.
- [9] Zou W, Lin M, Yang X, Zhang B. Ab initio calculations on the ground and low-lying excited states of InCl. *Journal of Chemical Physics* 2003;119:3721–8.
- [10] Schwerdtfeger P, Fischer T, Dolg M, Igel-Mann G, Nicklass A, Stoll H, et al. The accuracy of the pseudopotential approximation. I. An analysis of the spectroscopic constants for the electronic ground states of InCl and InCl₃ using various three valence electron pseudopotentials for indium. *Journal of Chemical Physics* 1995;102:2050–62.
- [11] Körber A, Hayashi D. Absorption and emission spectra of gaseous indium monohalides. XXVIII Int Conf on Phenomena in Ionized Gases (Prague) 2007;:1224–7.
- [12] Briefi S. Note: Implementation of a cold spot setup for controlled variation of vapor pressures and its application to an InBr containing discharge lamp. *Review of Scientific Instruments* 2013;84(2):026106 (pages 3).

Appendix

Table A.1: Franck-Condon factors for the A – X transition, part 1 (from $v'' = 0$ to $v'' = 12$).

v'	$v'' = 0$	$v'' = 1$	$v'' = 2$	$v'' = 3$	$v'' = 4$	$v'' = 5$	$v'' = 6$	$v'' = 7$	$v'' = 8$	$v'' = 9$	$v'' = 10$	$v'' = 11$	$v'' = 12$
0	0.546 39	0.309 92	0.107 03	0.028 69	0.006 42	0.001 28	0.000 22	0.000 03	0	0	0	0	0
1	0.356 05	0.093 66	0.274 88	0.178 29	0.070 03	0.020 71	0.005 09	0.001 06	0.000 20	0.000 03	0	0	0
2	0.087 59	0.386 37	0.000 46	0.167 42	0.195 46	0.107 07	0.040 12	0.011 88	0.002 89	0.000 61	0.000 11	0.000 02	0
3	0.009 54	0.180 74	0.309 83	0.025 40	0.078 06	0.175 84	0.131 01	0.060 73	0.021 17	0.005 93	0.001 41	0.000 29	0.000 05
4	0.000 39	0.027 99	0.252 88	0.216 72	0.072 04	0.025 28	0.139 43	0.140 55	0.079 06	0.032 06	0.010 17	0.002 70	0.000 60
5	0	0.001 37	0.051 99	0.300 58	0.138 76	0.107 94	0.003 15	0.100 44	0.137 91	0.093 26	0.043 30	0.015 42	0.004 52
6	0	0	0.002 87	0.078 25	0.328 38	0.082 73	0.126 73	0.000 75	0.066 36	0.127 11	0.102 38	0.053 96	0.021 35
7	0	0	0	0.004 66	0.104 35	0.342 49	0.046 16	0.131 18	0.008 65	0.040 06	0.111 85	0.106 58	0.063 32
8	0	0	0	0	0.006 43	0.128 73	0.348 55	0.024 07	0.126 05	0.020 42	0.021 71	0.094 87	0.106 80
9	0	0	0	0.000 01	0	0.007 87	0.150 50	0.350 87	0.011 70	0.115 60	0.032 30	0.010 06	0.078 34
10	0	0	0	0	0.000 03	0.000 05	0.008 71	0.169 16	0.352 45	0.005 34	0.102 86	0.042 49	0.003 55
11	0	0	0	0	0	0.000 06	0.000 16	0.008 79	0.184 37	0.355 37	0.002 37	0.089 74	0.050 37
12	0	0	0	0	0	0	0.000 10	0.000 43	0.008 04	0.195 84	0.360 87	0.001 15	0.077 31
13	0	0	0	0	0	0	0	0.000 14	0.000 90	0.006 53	0.203 28	0.369 71	0.000 78
14	0	0	0	0	0	0	0	0	0.000 17	0.001 64	0.004 50	0.206 33	0.382 14
15	0	0	0	0	0	0	0	0	0	0.000 19	0.002 71	0.002 34	0.204 50
16	0	0	0	0	0	0	0	0	0	0.000 02	0.000 18	0.004 07	0.000 61
17	0	0	0	0	0	0	0	0	0	0	0.000 04	0.000 13	0.005 66
18	0	0	0	0	0	0	0	0	0	0	0	0.000 08	0.000 06
19	0	0	0	0	0	0	0	0	0	0	0	0	0.000 13
20	0	0	0	0	0	0	0	0	0	0	0	0	0
21	0	0	0	0	0	0	0	0	0	0	0	0	0
22	0	0	0	0	0	0	0	0	0	0	0	0	0
23	0	0	0	0	0	0	0	0	0	0	0	0	0
24	0	0	0	0	0	0	0	0	0	0	0	0	0

Table A.2: Franck-Condon factors for the A – X transition, part 2 (from $v'' = 13$ to $v'' = 24$).

v'	$v'' = 13$	$v'' = 14$	$v'' = 15$	$v'' = 16$	$v'' = 17$	$v'' = 18$	$v'' = 19$	$v'' = 20$	$v'' = 21$	$v'' = 22$	$v'' = 23$	$v'' = 24$
0	0	0	0	0	0	0	0	0	0	0	0	0
1	0	0	0	0	0	0	0	0	0	0	0	0
2	0	0	0	0	0	0	0	0	0	0	0	0
3	0	0	0	0	0	0	0	0	0	0	0	0
4	0.000 11	0.000 02	0	0	0	0	0	0	0	0	0	0
5	0.001 10	0.000 22	0.000 04	0	0	0	0	0	0	0	0	0
6	0.006 85	0.001 80	0.000 40	0.000 07	0	0	0	0	0	0	0	0
7	0.027 56	0.009 63	0.002 74	0.000 64	0.000 13	0.000 02	0	0	0	0	0	0
8	0.070 79	0.033 77	0.012 71	0.003 88	0.000 98	0.000 20	0.000 03	0	0	0	0	0
9	0.103 77	0.076 43	0.039 55	0.016 02	0.005 21	0.001 40	0.000 31	0.000 05	0	0	0	0
10	0.063 31	0.098 64	0.080 15	0.044 76	0.019 38	0.006 69	0.001 91	0.000 44	0.000 07	0	0	0
11	0.000 63	0.050 33	0.092 29	0.082 09	0.049 31	0.022 63	0.008 28	0.002 49	0.000 60	0.000 11	0.000 01	0
12	0.055 94	0.000 01	0.039 62	0.085 24	0.082 75	0.052 96	0.025 77	0.009 89	0.003 13	0.000 79	0.000 15	0.000 02
13	0.065 99	0.059 58	0.000 70	0.030 94	0.078 25	0.082 10	0.055 95	0.028 55	0.011 55	0.003 80	0.001 00	0.000 20
14	0.000 90	0.055 94	0.061 70	0.002 01	0.024 15	0.071 46	0.080 74	0.058 06	0.031 10	0.013 10	0.004 51	0.001 23
15	0.398 10	0.001 56	0.047 07	0.062 79	0.003 45	0.018 92	0.065 22	0.078 76	0.059 51	0.033 27	0.014 57	0.005 20
16	0.197 37	0.417 11	0.003 11	0.039 19	0.063 26	0.004 73	0.014 94	0.059 64	0.076 40	0.060 36	0.035 04	0.015 92
17	0.000 01	0.184 58	0.438 31	0.006 15	0.032 11	0.063 48	0.005 68	0.011 97	0.054 73	0.073 88	0.060 64	0.036 50
18	0.007 30	0.001 34	0.166 09	0.460 31	0.011 47	0.025 64	0.063 77	0.006 19	0.009 77	0.050 57	0.071 25	0.060 56
19	0	0.008 74	0.005 36	0.142 24	0.481 21	0.019 93	0.019 66	0.064 41	0.006 25	0.008 15	0.047 09	0.068 65
20	0.000 19	0.000 04	0.009 65	0.012 68	0.114 09	0.498 54	0.032 39	0.014 14	0.065 66	0.005 88	0.006 96	0.044 24
21	0	0.000 24	0.000 28	0.009 71	0.023 54	0.083 49	0.509 35	0.049 52	0.009 15	0.067 78	0.005 11	0.006 08
22	0	0.000 01	0.000 27	0.000 83	0.008 71	0.037 59	0.053 17	0.510 51	0.071 57	0.004 91	0.071 03	0.004 05
23	0	0	0.000 03	0.000 25	0.001 78	0.006 69	0.053 78	0.026 61	0.499 15	0.098 13	0.001 76	0.075 71
24	0	0	0	0.000 08	0.000 19	0.003 15	0.004 01	0.070 32	0.007 70	0.473 14	0.127 88	0.000 13

Table A.3: Franck-Condon factors for the B – X transition, part 1 (from $v'' = 0$ to $v'' = 12$).

v'	$v'' = 0$	$v'' = 1$	$v'' = 2$	$v'' = 3$	$v'' = 4$	$v'' = 5$	$v'' = 6$	$v'' = 7$	$v'' = 8$	$v'' = 9$	$v'' = 10$	$v'' = 11$	$v'' = 12$
0	0.603 96	0.287 05	0.085 06	0.019 55	0.003 68	0.000 61	0.000 08	0	0	0	0	0	0
1	0.327 92	0.162 49	0.292 40	0.152 41	0.049 73	0.012 18	0.002 43	0.000 39	0.000 05	0	0	0	0
2	0.063 38	0.400 87	0.022 22	0.218 82	0.183 49	0.079 97	0.024 30	0.005 71	0.001 07	0.000 16	0.000 02	0	0
3	0.004 64	0.136 24	0.376 34	0.000 43	0.141 51	0.185 78	0.104 17	0.037 93	0.010 37	0.002 18	0.000 37	0.000 04	0
4	0.000 07	0.013 21	0.199 97	0.323 63	0.017 43	0.082 38	0.171 32	0.120 14	0.051 38	0.015 94	0.003 75	0.000 69	0.000 09
5	0	0.000 19	0.023 65	0.250 78	0.270 89	0.040 97	0.043 36	0.149 44	0.128 50	0.063 24	0.021 99	0.005 69	0.001 15
6	0	0	0.000 27	0.034 02	0.290 13	0.227 91	0.059 69	0.020 17	0.126 28	0.130 67	0.072 99	0.027 93	0.007 93
7	0	0	0.000 04	0.000 25	0.042 79	0.320 80	0.196 80	0.071 03	0.007 79	0.104 94	0.128 71	0.080 24	0.033 56
8	0	0	0	0.000 11	0.000 13	0.048 90	0.345 40	0.176 96	0.075 51	0.002 08	0.086 86	0.124 04	0.085 29
9	0	0	0	0	0.000 24	0	0.051 67	0.365 67	0.167 12	0.074 52	0.000 16	0.072 31	0.118 08
10	0	0	0	0	0	0.000 45	0.000 10	0.050 71	0.382 37	0.166 27	0.069 44	0.000 16	0.061 15
11	0	0	0	0	0	0	0.000 73	0.000 74	0.046 00	0.395 41	0.173 75	0.061 42	0.001 02
12	0	0	0	0	0	0	0	0.001 03	0.002 29	0.037 92	0.403 81	0.189 30	0.051 36
13	0	0	0	0	0	0	0	0	0.001 28	0.005 09	0.027 41	0.405 90	0.212 83
14	0	0	0	0	0	0	0	0.000 01	0.000 04	0.001 36	0.009 31	0.016 04	0.399 37
15	0	0	0	0	0	0	0	0	0.000 02	0.000 12	0.001 20	0.014 80	0.006 09
16	0	0	0	0	0	0	0	0	0	0.000 02	0.000 29	0.000 78	0.020 98
17	0	0	0	0	0	0	0	0	0	0	0.000 01	0.000 56	0.000 26
18	0	0	0	0	0	0	0	0	0	0	0.000 01	0	0.000 89
19	0	0	0	0	0	0	0	0	0	0	0	0.000 02	0
20	0	0	0	0	0	0	0	0	0	0	0	0	0.000 02
21	0	0	0	0	0	0	0	0	0	0	0	0	0
22	0	0	0	0	0	0	0	0	0	0	0	0	0
23	0	0	0	0	0	0	0	0	0	0	0	0	0
24	0	0	0	0	0	0	0	0	0	0	0	0	0

Table A.4: Franck-Condon factors for the B – X transition, part 2 (from $v'' = 13$ to $v'' = 24$).

v'	$v'' = 13$	$v'' = 14$	$v'' = 15$	$v'' = 16$	$v'' = 17$	$v'' = 18$	$v'' = 19$	$v'' = 20$	$v'' = 21$	$v'' = 22$	$v'' = 23$	$v'' = 24$
0	0	0	0	0	0	0	0	0	0	0	0	0
1	0	0	0	0	0	0	0	0	0	0	0	0
2	0	0	0	0	0	0	0	0	0	0	0	0
3	0	0	0	0	0	0	0	0	0	0	0	0
4	0	0	0	0	0	0	0	0	0	0	0	0
5	0.000 16	0.000 01	0	0	0	0	0	0	0	0	0	0
6	0.001 71	0.000 26	0.000 02	0	0	0	0	0	0	0	0	0
7	0.010 24	0.002 38	0.000 38	0.000 04	0	0	0	0	0	0	0	0
8	0.038 47	0.012 58	0.003 08	0.000 52	0.000 05	0	0	0	0	0	0	0
9	0.088 30	0.042 64	0.014 72	0.003 82	0.000 67	0.000 07	0	0	0	0	0	0
10	0.111 58	0.089 80	0.045 87	0.016 67	0.004 51	0.000 83	0.000 09	0	0	0	0	0
11	0.052 94	0.105 20	0.090 04	0.048 24	0.018 29	0.005 13	0.000 97	0.000 11	0	0	0	0
12	0.002 17	0.047 28	0.099 18	0.089 43	0.049 76	0.019 58	0.005 65	0.001 10	0.000 12	0	0	0
13	0.040 03	0.003 35	0.043 84	0.093 70	0.088 17	0.050 52	0.020 48	0.006 05	0.001 19	0.000 13	0	0.000 01
14	0.244 13	0.028 27	0.004 53	0.042 38	0.088 73	0.086 50	0.050 61	0.020 98	0.006 31	0.001 25	0.000 13	0
15	0.381 79	0.282 46	0.017 06	0.005 77	0.042 86	0.084 12	0.084 67	0.050 02	0.021 16	0.006 40	0.001 29	0.000 12
16	0.000 41	0.351 07	0.326 11	0.007 64	0.007 22	0.045 32	0.079 73	0.082 73	0.048 90	0.020 95	0.006 39	0.001 26
17	0.026 73	0.002 09	0.306 26	0.372 03	0.001 49	0.009 08	0.050 05	0.075 23	0.080 90	0.047 21	0.020 46	0.006 20
18	0	0.030 57	0.013 84	0.248 32	0.415 48	0.000 23	0.011 61	0.057 49	0.070 33	0.079 30	0.045 00	0.019 72
19	0.001 19	0.000 56	0.030 90	0.036 95	0.181 15	0.450 10	0.005 26	0.015 08	0.068 30	0.064 67	0.078 09	0.042 27
20	0.000 05	0.001 32	0.002 55	0.026 73	0.070 29	0.112 00	0.468 40	0.017 35	0.019 76	0.083 32	0.057 96	0.077 52
21	0.000 02	0.000 18	0.001 14	0.006 34	0.018 39	0.109 37	0.051 19	0.463 17	0.036 04	0.025 79	0.103 53	0.049 96
22	0	0.000 02	0.000 43	0.000 64	0.011 66	0.008 28	0.146 29	0.010 63	0.429 35	0.059 11	0.032 96	0.129 86
23	0	0.000 01	0	0.000 76	0.000 11	0.017 27	0.000 91	0.170 93	0.000 89	0.366 27	0.082 46	0.040 54
24	0	0	0.000 02	0.000 01	0.001 05	0.000 14	0.021 10	0.001 97	0.173 75	0.027 19	0.279 89	0.100 55

Table A.5: Transition probabilities $A_{ik}^{v'v''}$ (s^{-1}) for the A – X transition, part 1 (from $v'' = 0$ to $v'' = 12$).

v'	$v'' = 0$	$v'' = 1$	$v'' = 2$	$v'' = 3$	$v'' = 4$	$v'' = 5$	$v'' = 6$	$v'' = 7$	$v'' = 8$	$v'' = 9$	$v'' = 10$	$v'' = 11$	$v'' = 12$
0	90 202	40 403	11 117	2373	414	64	8	0	0	0	0	0	0
1	74 083	16 386	36 689	18 893	5901	1367	260	40	5	0	0	0	0
2	23 201	82 794	167	22 938	21 111	9191	2702	621	111	16	2	0	0
3	3332	49 079	68 670	3778	11 047	19 349	11 438	4169	1128	234	40	5	0
4	199	10 034	70 451	50 020	11 527	3769	15 620	12 476	5516	1744	410	78	11
5	3	730	19 140	85 981	33 722	17 817	550	11 462	12 419	6615	2393	637	135
6	0	9	1604	29 602	96 538	21 552	21 352	61	7716	11 601	7365	3028	900
7	0	0	15	2740	40 583	103 580	13 272	22 438	1065	4752	10 337	7758	3607
8	0	0	2	18	3997	51 500	108 570	8014	21 792	2691	2640	8858	7867
9	0	0	0	6	13	5208	61 982	112 660	4871	20 111	4400	1264	7386
10	0	0	0	0	14	3	6205	71 771	116 760	3114	17 909	5923	473
11	0	0	0	0	0	30	2	6840	80 660	121 540	2232	15 523	7157
12	0	0	0	0	0	0	54	34	6997	88 441	127 450	1912	13 161
13	0	0	0	0	0	0	0	88	140	6612	94 888	134 830	2024
14	0	0	0	0	0	0	0	0	127	368	5692	99 703	143 850
15	0	0	0	0	0	0	0	0	0	166	772	4333	102 510
16	0	0	0	0	0	0	0	0	1	3	193	1388	2733
17	0	0	0	0	0	0	0	0	0	2	10	194	2231
18	0	0	0	0	0	0	0	0	0	0	2	26	163
19	0	0	0	0	0	0	0	0	0	0	0	3	54
20	0	0	0	0	0	0	0	0	0	0	0	0	2
21	0	0	0	0	0	0	0	0	0	0	0	0	2
22	0	0	0	0	0	0	0	0	0	0	0	0	0
23	0	0	0	0	0	0	0	0	0	0	0	0	0
24	0	0	0	0	0	0	0	0	0	0	0	0	0

Table A.6: Transition probabilities $A_{ik}^{v'v''}$ (s^{-1}) for the A – X transition, part 2 (from $v'' = 13$ to $v'' = 24$).

v'	$v'' = 13$	$v'' = 14$	$v'' = 15$	$v'' = 16$	$v'' = 17$	$v'' = 18$	$v'' = 19$	$v'' = 20$	$v'' = 21$	$v'' = 22$	$v'' = 23$	$v'' = 24$
0	0	0	0	0	0	0	0	0	0	0	0	0
1	0	0	0	0	0	0	0	0	0	0	0	0
2	0	0	0	0	0	0	0	0	0	0	0	0
3	0	0	0	0	0	0	0	0	0	0	0	0
4	0	0	0	0	0	0	0	0	0	0	0	0
5	21	2	0	0	0	0	0	0	0	0	0	0
6	209	36	4	0	0	0	0	0	0	0	0	0
7	1179	301	56	7	0	0	0	0	0	0	0	0
8	4077	1472	404	81	11	0	0	0	0	0	0	0
9	7711	4455	1744	519	111	17	1	0	0	0	0	0
10	6016	7385	4715	1997	638	145	24	2	0	0	0	0
11	101	4807	6958	4858	2227	752	184	32	3	0	0	0
12	8088	0	3800	6449	4933	2404	869	222	42	4	0	0
13	10 906	8772	58	2967	5945	4904	2565	965	265	51	5	0
14	2582	8807	9266	192	2311	5433	4837	2668	1061	302	62	6
15	154 570	3723	6864	9654	340	1797	4956	4721	2740	1139	338	73
16	102 910	166 870	5697	5074	10 013	464	1399	4525	4572	2782	1201	371
17	1207	100 480	180 450	8843	3447	10 419	542	1097	4138	4411	2786	1255
18	3265	176	94 895	194 750	13 579	2016	10 957	557	864	3810	4230	2775
19	101	4396	142	85 970	208 880	20 355	866	11 717	507	683	3536	4042
20	96	32	5455	1623	73 854	221 670	29 591	142	12 802	400	538	3313
21	0	147	0	6224	5045	59 104	231 550	41 580	63	14 345	252	415
22	3	0	200	83	6468	10 616	42 818	236 830	56 372	927	16 511	101
23	0	5	5	238	368	6020	18 186	26 643	235 780	73 608	3092	19 503
24	0	0	5	20	244	930	4850	27 148	12 670	226 990	92 393	6924

Table A.8: Transition probabilities $A_{ik}^{v'v''}$ (s^{-1}) for the B – X transition, part 2 (from $v'' = 13$ to $v'' = 24$).

v'	$v'' = 13$	$v'' = 14$	$v'' = 15$	$v'' = 16$	$v'' = 17$	$v'' = 18$	$v'' = 19$	$v'' = 20$	$v'' = 21$	$v'' = 22$	$v'' = 23$	$v'' = 24$
0	0	0	0	0	0	0	0	0	0	0	0	0
1	0	0	0	0	0	0	0	0	0	0	0	0
2	0	0	0	0	0	0	0	0	0	0	0	0
3	0	0	0	0	0	0	0	0	0	0	0	0
4	1	0	0	0	0	0	0	0	0	0	0	0
5	28	2	0	0	0	0	0	0	0	0	0	0
6	307	45	4	0	0	0	0	0	0	0	0	0
7	1904	428	66	6	0	0	0	0	0	0	0	0
8	7398	2342	555	91	9	0	0	0	0	0	0	0
9	17 550	8209	2745	689	118	12	0	0	0	0	0	0
10	22 904	17 860	8839	3112	815	145	15	0	0	0	0	0
11	11 213	21 599	17 918	9303	3418	929	170	18	0	0	0	0
12	473	10 014	20 364	17 800	9600	3661	1024	193	20	0	1	1
13	9008	732	9279	19 233	17 548	9748	3831	1096	210	22	0	2
14	56 563	6354	988	8965	18 204	17 211	9764	3926	1145	220	22	0
15	91 003	65 337	3828	1257	9057	17 245	16 837	9647	3959	1162	226	21
16	100	83 509	75 293	1711	1570	9565	16 328	16 439	9427	3918	1159	222
17	6729	512	72 681	85 714	334	1972	10 546	15 387	16 057	9093	3825	1125
18	0	7673	3373	58 780	95 500	51	2516	12 093	14 361	15 718	8658	3683
19	317	144	7731	8981	42 761	103 190	1172	3261	14 338	13 182	15 455	8122
20	13	348	655	6665	17 028	26 357	107 080	3853	4262	17 452	11 790	15 313
21	7	50	299	1620	4569	26 403	12 008	105 550	7979	5546	21 631	10 138
22	2	4	116	168	2968	2049	35 185	2485	97 518	13 046	7069	27 057
23	0	4	0	205	28	4380	223	40 948	206	82 892	18 137	8667
24	0	0	6	3	282	35	5326	483	41 447	6306	63 097	22 034